Effects of Alpha-ion Stopping on Ignition and Ignition Criteria in Inertial Confinement Fusion Experiments

Benjamin Reichelt,[1] Richard Petrasso,[1] and Chikang Li[1]
Massachusetts Institute of Technology, Cambridge, Massachusetts 02139, USA

(*The author to whom correspondence may be addressed: Benjamin Reichelt, blr@mit.edu)

(Dated: 17 January 2024)

With the advent of ignited plasmas at the National Ignition Facility (NIF), alpha physics has become a driving factor in theoretical understanding and experimental behavior. In this communication, we explore aspects of direct alpha-ion heating through comparison of the consequences from the one-fluid and two-fluid models in the hydrodynamic approach. We show that the case with all alpha energy deposited in electrons raises the ignition criteria by $\sim 4keV$ or $\sim 0.2g/cm^2$ in the hot spot relative to the case with all alpha energy deposited in ions. In the case of the recently ignited NIF implosion, 30% of the 3.5 MeV α energy is deposited into the DT fuel ions, for which there is negligible difference between the one-fluid and two-fluid ignition criteria. However, changes in the ion stopping fraction through profile effects and alternate stopping power models could lead to ignition curve shifts of $\sim 1keV$.

Recently, the National Ignition Facility (NIF) achieved its long sought and eponymous goal of ignition for an Inertial Confinement Fusion (ICF) experiment[1–3]. This entails coupling more power from fusion into the hot spot than escapes via bremsstrahlung, conduction, and pdV expansion work so that a self propagating burn wave is produced and grows until the capsule is disassembled by outward expansion.

The standard formulation for ignition criteria in a hydrodynamic regime often involves a simple one-fluid model where bremsstrahlung and other losses and sources of fusion power and compressive work act upon the same fluid[1,4]. In this context, we begin with the system of equations developed in ref[4]:

$$\begin{aligned} \frac{dE}{dt} &= P_f - P_b - P_c - 4\pi R^2 u p_s \\ \frac{dN}{dt} &= \frac{((1-f_{hs})P_f + P_c)}{3T} \\ \frac{dR}{dt} &= u \end{aligned} \tag{1}$$

Where E is the total internal energy of the hot spot, N is the number of DT atoms in the hot spot (which is equal to the number of electrons), and R is the hot spot radius. u is a velocity characterizing the expansion of the hot spot through burn wave propagation, p_s is the stagnation pressure, and P_f, P_c, and P_b are power losses/gains through fusion alphas, conduction, and bremsstrahlung respectively. Finally, f_{hs} is a number representing the fraction of alpha energy deposited in the hot spot and $T = (2/3)E/N$ is the temperature in the hot spot.

Note that equation 1 can be split into a separate ion and electron fluid that behave identically, like so:

$$\begin{aligned} \frac{dE_i}{dt} &= P_f/2 - P_b/2 - P_c/2 - 4\pi R^2 u p_s/2 \\ \frac{dE_e}{dt} &= \frac{dE_i}{dt} \\ \frac{dN}{dt} &= \frac{2((1-f_{hs})P_f + P_c)}{3(T_i + T_e)} \\ \frac{dR}{dt} &= u \end{aligned} \tag{2}$$

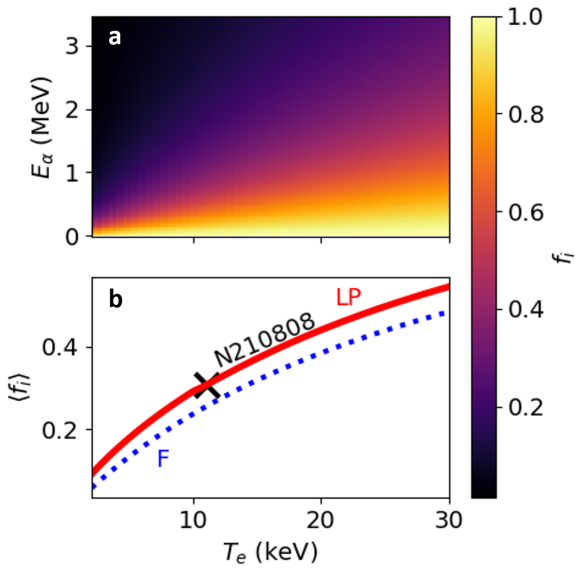

FIG. 1. Fraction of energy f_i deposited by alphas into DT plasma ions, assuming $n_{DT} = 10^{26} cm^{-3}$ a) plotted vs alpha energy and electron temperature for the LP model b) averaged over a 3.5 MeV DT alpha stopping trajectory in solid red and a model from ref[5] in dotted blue and labeled F. The marked point shows the averaged $\langle f_i \rangle$ for the first igniting NIF shot N210808 on the LP curve. This indicates that a non-negligible amount of fusion power couples directly into ions and that there is a large variation in the extent of this coupling as hot spot conditions change.

Such that $E = E_i + E_e$ and $T_{i(e)} = (2/3)E_{i(e)}/N$, where i subscripts denote the ion fluid and e subscripts the electron fluid. This splitting at the moment does not change the dynamics at all, since the ions are forced to behave identically to the electrons– it does, however, provide a useful comparison to the two-fluid case where ions and electrons behave separately.

In reality, bremsstrahlung and conduction losses are mostly confined to the electron fluid, while energy addition through

alpha stopping can go into both an alpha-ion channel and alpha-electron. The alpha-electron channel is the most commonly mentioned one in the context of ICF ignition research, but alpha-ion stopping becomes more and more important as electron temperatures increase because electron thermal speed becomes more disparate from the alpha velocity[4–6]. This can be seen in fig 1 a, where the ion fraction of alpha stopping power $f_i = (dE/dx)^{\alpha\to i}/(dE/dx)^{tot}$ is plotted versus alpha energy and electron temperature given the LP stopping model[6]:

$$\frac{dE^{t\to f}}{dx} = -\left(\frac{Z_t e\omega_{pf}}{v_t}\right)^2 ln\Lambda_b \times\left[\mu - \frac{m_f}{m_t}\left[\frac{d\mu}{d\zeta} - \frac{1}{ln\Lambda_b}\left[\mu + \frac{d\mu}{d\zeta}\right]\right]\right] \tag{3}$$

Where $dE^{t\to f}/dx$ is the stopping power of test particle t on a field of species f, Z_t is the charge of t, ω_{pf} is the plasma frequency of f, $v_{t(f)}$ is the velocity of $t(f)$, $ln\Lambda_b$ is the coulomb log of $t\to f$ collisions, $\zeta = v_t^2/v_f^2$, $\mu(\zeta) = 2\int_0^\zeta exp(-\xi)\sqrt{\xi}d\xi/\sqrt{\pi}$ is the maxwell integral, and $m_{t(f)}$ is the test (field) particle mass.

In fig 1 b, this fraction has been averaged over the alpha stopping trajectory to get $\langle f_i\rangle$, the average ion stopping fraction over a uniform hot spot. The resulting curve reveals that for ignition relevant capsules, a significant fraction of the energy is deposited through the alpha-ion channel. Since ion energy is directly coupled to fusion power but not directly coupled to two of the loss mechanisms, this could potentially have discernible impacts on ignition dynamics. Other ion stopping power models have been studied before– one such example being indicated on fig 1 b from ref[5], which uses a first order expansion of the collision operator as opposed to the second order expansion from ref[6]. While some past works of ICF modeling explored alpha-ion physics through a kinetic[7,8] or hybrid approach[9], direct illustration of the effect of alpha-ion stopping in isolation using a hydrodynamic approach is lacking.

To determine the extent of these effects, we alter the model of eqns 2 by separating these dynamics to the appropriate fluid and introducing an ion-electron equilibration term[10]:

$$\begin{aligned}\frac{dE_i}{dt} &= P_f\langle f_i\rangle - 4\pi R^2 u p_s/2 + \frac{3}{2}N\nu(T_e - T_i)\\ \frac{dE_e}{dt} &= P_f(1-\langle f_i\rangle) - P_b - P_c - 4\pi R^2 u p_s/2 + \frac{3}{2}N\nu(T_i - T_e)\\ \frac{dN}{dt} &= \frac{2((1-f_{hs})P_f + P_c)}{3(T_i+T_e)}\\ \frac{dR}{dt} &= u\end{aligned} \tag{4}$$

The new parameter ν is the temperature equilibration frequency for electrons and ions (ion-ion and electron-electron times are orders of magnitude faster and neglected here). $\nu^{-1} \approx 10ps$ for the conditions in the N210808 hot spot[1,2], which is less than but a similar order to the burn width ($\sim 90ps$) and thus can have noticeable effects on dynamics. To probe this, a system of differential equations with the form of eqns 2 and 4 were solved using the Adams/BDF method[11,12], with expressions for P_f, P_b, P_c, f_{hs} and ν taken from refs[4,13]:

$$\begin{aligned}P_f &= \left(\frac{N}{2V}\right)^2 V E_{\alpha 0}\beta_f T_i^{-2/3} exp(-19.94 T_{i,keV}^{-1/3})\\ P_b &= \beta_b * \left(\frac{N}{V}\right)^2 T_e^{1/2} V\\ P_c &= \frac{3A_e T_e^{7/2}}{ln\Lambda_{ee} R^2} V\\ f_{hs} &= \begin{cases}\frac{3}{2}\tau_\alpha - \frac{4}{5}\tau_\alpha^2, & \tau_\alpha \le 1/2\\ 1 - \frac{1}{4\tau_\alpha} - \frac{1}{160\tau_\alpha^3}, & \tau_\alpha > 1/2\end{cases}\\ \nu &= \frac{\beta_\nu (m_{DT} m_e)^{1/2}(N/V) ln\Lambda_{ie}}{(m_{DT}T_e + m_e T_i)^{3/2}}\end{aligned} \tag{5}$$

Where β_f, β_b, A_e, and β_ν are unitful constants, $E_{\alpha 0}$ is the initial DT α kinetic energy, V is hot spot volume, $m_{DT(e)}$ is the average DT (electron) mass, and $\tau_\alpha \approx 9 ln\Lambda_{\alpha e}(\rho R)_{hs,g/cm^2}/T_{e,keV}^{3/2}$ is the ratio of hot spot radius to alpha range in the hot spot.

The burn wave was assumed to behave as a strong shock following ref[4], yielding $u = 0.2\mu m/ps$. Initial conditions were taken from experimental values of NIF shot N210307[14,15], which did not ignite. Additionally, to account for the fact that the experimental values of N210808 are taken in a burn averaged sense over an igniting plasma, and thus aren't the most relevant for initial conditions, a synthetic set of data are also used with intermediate conditions between N210808 and N210307. A summary of the various initial conditions is given in table I.

Fig 2 shows the dynamic values of several variables vs time given the initial conditions described above. Within these simulations, only p_s and u are fixed, while other variables like $\langle f_i\rangle$ are functions of the state of the capsule. Most strikingly, with the synthetic intermediate data used, the one-fluid model indicates ignition via a rapid temperature and density rise, while the two-fluid model does not. Thus, there are regions of parameter space where experiments approaching the igniting conditions of N210808 would be predicted to ignite with the one-fluid model but not with the two-fluid model. Additionally, we can see measurable differences $\gtrsim 10ps$ between the burn initiation time for one-fluid and two-fluid models. Thus, precisely measuring the bang time and width of the burn should help to elucidate the relationships between ion and electron temperatures and the increasing rate of alpha-ion deposition as temperatures increase.

To further probe the effect of direct alpha-ion stopping $\langle f_i\rangle$ is held artificially constant in this model. So as to avoid confusion with the dynamic value from before, we denote the constant stopping fraction by $\langle f_i\rangle_c$ hereafter. The results from such a setup are shown in fig 3, which shows the burn history

TABLE I. Initial conditions simulated, taken from ref[1,2] (the electron temperature is assumed equal to the ion temperature initially due to lack of a measurement)

Initial Conditions	V_{hs} [$10^3 \mu m^3$]	ρR_{hs} [g/cm^2]	p_{hs} [Gbar]	$T_{i,hs}$ [keV]	$T_{e,hs}$ [keV]
N210808	640	0.44	569	11	11
Synthetic	270	0.44	400	7.5	7.5
N210307	270	0.38	353	5	5

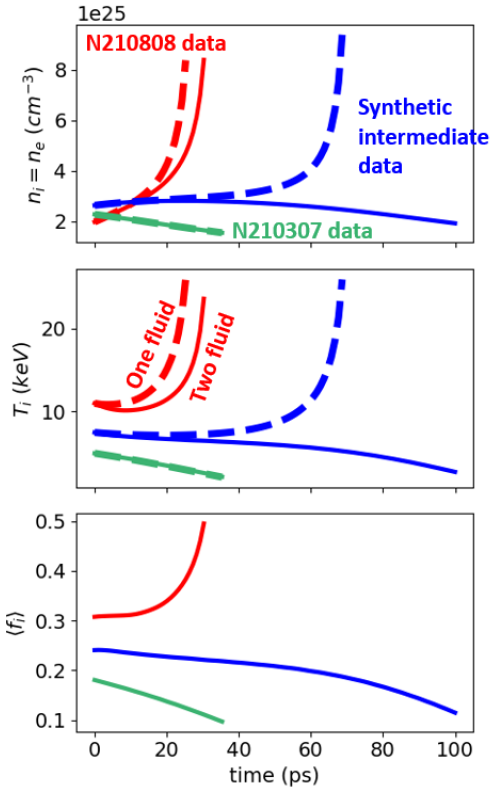

FIG. 2. Dynamic quantities for the 1 fluid (dashed lines) and 2 fluid (solid lines) models given a variety of initial conditions. This indicates that generally the single fluid model predicts that ignition boundary occurs at higher temperatures and densities for the standard model as compared to a more physical two-fluid model.

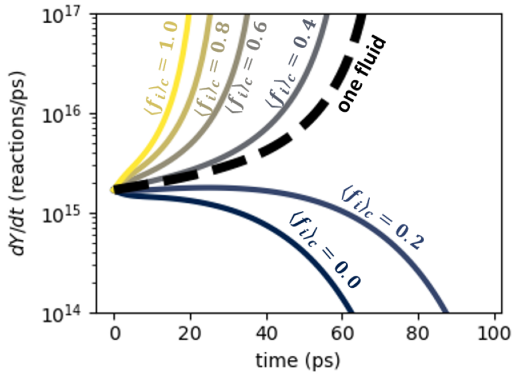

FIG. 3. Burn histories for two-fluid (solid colored lines) and one-fluid (dashed black line) models, given synthetic initial conditions in table I. These curves demonstrate that ion coupling percentage has a strong impact on burn dynamics and that the model, for these conditions, behaves similarly to the two-fluid model with $\langle f_i \rangle_c = 0.4$.

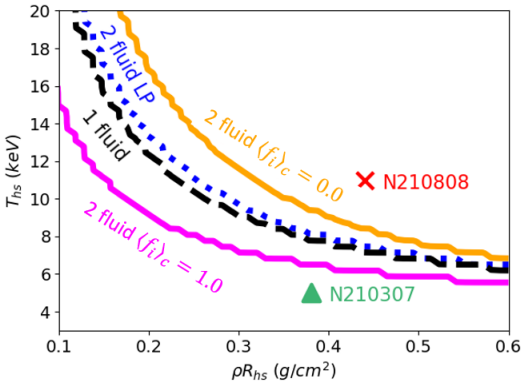

FIG. 4. Ignition criteria for an isobaric hot spot with several different ion stopping fraction models as compared to experimental conditions. One and two-fluid models with LP $\langle f_i \rangle$ behave similarly but there is a large difference between $\langle f_i \rangle_c = 0.0$ and $\langle f_i \rangle_c = 1.0$ criteria, indicating that in integrated hydro simulations it is important to include alpha-ion stopping.

for the intermediate synthetic initial conditions for a variety of fixed ion stopping fractions. It is seen that there is a strong sensitivity on ion stopping fraction for the two-fluid model, and that the one-fluid model performs about as well as the two-fluid model with $\langle f_i \rangle_c = 0.4$. This aligns with the fact that the model implicitly has $\langle f_i \rangle_c = 0.5$ from eqn 2. The slightly lower $\langle f_i \rangle$ required for the model to be equivalent to the two-fluid model is because the ion channel in the two-fluid model is shielded from direct energy losses. Overall, it is shown that the degree to which fusion energy couples directly to ions can have a notable affect on ignition dynamics and that the model behaves similarly to the two-fluid model with $\langle f_i \rangle_c$ fixed at 0.4.

Whilst other works exploring ignition criteria have implicitly or explicitly included two-fluid effects, they have either focused on a limited number of cases which are often out of date in terms of design[5,7], or they have utilized complicated integrated models that make it difficult to distinguish the influences of particular mechanisms[16].

As a more thorough study, a suite of simulations may be run

to get a sense of how the ignition boundary is shifted by two-fluid effects. This is demonstrated in fig 4, which shows how the ignition criteria changes for the two-fluid model under the two extremes of $\langle f_i \rangle_c = 0.0$ and $\langle f_i \rangle_c = 1.0$ as compared to the one-fluid model and the two-fluid LP model[6]. These simulations assume an isobaric hotspot with $p_{stag} = 2n_0T_0$, $V_{hs} = 3 \times 10^5 \mu m^3$, and $u = 0.2\mu m/ps$. The benefit of this model is that it has a low computational cost that easily allows for scans such as this one over large regions of parameter space. Fig 4 shows that the impact of two-fluid effects can be quite large, with the $\langle f_i \rangle_c = 0.0$ shifting ignition criteria up by $\sim 0.05 g/cm^2$ or $\sim 2keV$ relative to the one-fluid model for ignition relevant conditions. However, the difference between the one-fluid and two-fluid with LP alpha stopping is quite small, shifting the ignition boundary by significantly less: $\sim 0.02 g/cm$ or $\sim 0.3keV$. Thus the one-fluid and two-fluid models have little difference from each other and so the synthetic intermediate data demonstrated in fig 2, in reality, is exploring a small region in parameter space where the one-fluid model ignites but the 2 fluid LP model does not.

In contrast, the significant shift of the $\langle f_i \rangle_c = 0$ boundary with respect to $\langle f_i \rangle_c = 1$ demonstrates that careful inclusion of alpha-ion partitioning is important to model accurately in hydro simulations of ICF experiments. To this issue, there have been many burn physics packages developed for hydrodynamics codes that take into account nonlocal alpha transport effects using monte carlo techniques, and the work herein reinforces the fact that the choice of alpha stopping model may play a large part in the behavior of the simulations.

There are several simplifications in this model compared to a full hydro simulation. Profile effects could work to shift the ignition boundary up as alphas deposit energy into regions with lower temperatures and thus lower $\langle f_i \rangle$, shifting the ignition curve closer to the $\langle f_i \rangle_c = 0$ curve on fig 4. If the average temperature experienced by alphas is halved from 7.5 keV to 3.8 keV, $\langle f_i \rangle$ would drop from ~ 0.2 to ~ 0.1, leading to a further $\sim 1keV$ increase in the temperature required for ignition. This model also does not take into account re-absorption of radiation, which effectively serves to augment the electron heat conduction term since radiation is coupled to the electrons. Since this term has no $\langle f_i \rangle$ coupling, radiative transport may shift the absolute locations of the one-fluid and two-fluid curves but wouldn't be expected to significantly change the relative positioning of the curves. Finally, this model assumes instantaneous alpha transport, when in reality the alphas will take $\sim 10ps$ to stop[4,13]. This would likely shift ignition curves upward but this will affect the ion and electron channels similarly so the relative relationship between the 1 fluid and two-fluid curves will likely be preserved.

It is interesting to note that related transient dynamics may also be important for ignition criteria in magnetic fusion, although the exact model will differ. For instance, conditions on the planned SPARC tokomak lead to $\nu^{-1} \approx 1s$, on the same order as the pulse width[17], meaning that separate ion and electron dynamics may play a non-negligible role in achieving self heating through alphas.

To conclude, details of alpha-ion stopping are important physics to quantify in the new regime of igniting experiments where burn physics dominates, and it has, as might be conjectured, noticeable impacts on ignition criteria. A two-fluid model has been developed that indicates a $\sim 4keV$ shift upward in ignition criteria between the case with 100% of fusion energy coupled into ions vs 100% of fusion energy coupled into electrons. The recently ignited shot N210808 had 30% of the α energy deposited into the ions, a range in which the two-fluid model with LP stopping behaves quite similarly to the one-fluid model. Nevertheless, this model re-emphasizes the importance of taking into account alpha-ion stopping in hydro-codes and of doing so in an accurate manner since lower than expected ion stopping and profile effects could lead to notable shifts upward of the ignition boundary on the order of $1keV$.

ACKNOWLEDGMENTS

This work was supported in part by DOE/NNSA CoE contract DE-NA0003868; B. Reichelt is supported by NNSA SSGF DE-NA0003960.

[1] H. Abu-Shawareb, R. Acree, P. Adams, J. Adams, B. Addis, R. Aden, P. Adrian, B. Afeyan, M. Aggleton, L. Aghaian, *et al.*, "Lawson criterion for ignition exceeded in an inertial fusion experiment," Physical Review Letters **129**, 075001 (2022).

[2] A. Kritcher, A. Zylstra, D. Callahan, O. Hurricane, C. Weber, D. Clark, C. Young, J. Ralph, D. Casey, A. Pak, *et al.*, "Design of an inertial fusion experiment exceeding the lawson criterion for ignition," Physical Review E **106**, 025201 (2022).

[3] A. Zylstra, A. Kritcher, O. Hurricane, D. Callahan, J. Ralph, D. Casey, A. Pak, O. Landen, B. Bachmann, K. Baker, *et al.*, "Experimental achievement and signatures of ignition at the national ignition facility," Physical Review E **106**, 025202 (2022).

[4] S. Atzeni and J. Meyer-ter Vehn, *The physics of inertial fusion: beam plasma interaction, hydrodynamics, hot dense matter*, Vol. 125 (OUP Oxford, 2004).

[5] G. Fraley, E. Linnebur, R. Mason, and R. Morse, "Thermonuclear burn characteristics of compressed deuterium-tritium microspheres," The Physics of Fluids **17**, 474–489 (1974).

[6] C. K. Li and R. D. Petrasso, "Charged-particle stopping powers in inertial confinement fusion plasmas," Physical review letters **70**, 3059 (1993).

[7] B. Peigney, O. Larroche, and V. Tikhonchuk, "Ion kinetic effects on the ignition and burn of inertial confinement fusion targets: A multi-scale approach," Physics of Plasmas **21** (2014).

[8] B. Appelbe, M. Sherlock, O. El-Amiri, C. Walsh, and J. Chittenden, "Modification of classical electron transport due to collisions between electrons and fast ions," Physics of Plasmas **26** (2019).

[9] C.-K. Huang, K. Molvig, B. J. Albright, E. S. Dodd, E. L. Vold, G. Kagan, and N. M. Hoffman, "Study of the ion kinetic effects in icf run-away burn using a quasi-1d hybrid model," Physics of Plasmas **24** (2017).

[10] S. Braginskii, "Review of plasma physics 1, ed. by acad," MA Leontovich, Consultants Bureau, New York (1965).

[11] P. Virtanen, R. Gommers, T. E. Oliphant, M. Haberland, T. Reddy, D. Cournapeau, E. Burovski, P. Peterson, W. Weckesser, J. Bright, S. J. van der Walt, M. Brett, J. Wilson, K. J. Millman, N. Mayorov, A. R. J. Nelson, E. Jones, R. Kern, E. Larson, C. J. Carey, İ. Polat, Y. Feng, E. W. Moore, J. VanderPlas, D. Laxalde, J. Perktold, R. Cimrman, I. Henriksen, E. A. Quintero, C. R. Harris, A. M. Archibald, A. H. Ribeiro, F. Pedregosa, P. van Mulbregt, and SciPy 1.0 Contributors, "SciPy 1.0: Fundamental Algorithms for Scientific Computing in Python," Nature Methods **17**, 261–272 (2020).

[12] L. Petzold, "Automatic selection of methods for solving stiff and nonstiff systems of ordinary differential equations," SIAM journal on scientific and statistical computing **4**, 136–148 (1983).

[13] J. D. Huba, *NRL plasma formulary*, Vol. 6790 (Naval Research Laboratory, 1998).
[14] A. Zylstra, O. Hurricane, D. Callahan, A. Kritcher, J. Ralph, H. Robey, J. Ross, C. Young, K. Baker, D. Casey, *et al.*, "Burning plasma achieved in inertial fusion," Nature **601**, 542–548 (2022).
[15] A. Kritcher, C. Young, H. Robey, C. Weber, A. Zylstra, O. Hurricane, D. Callahan, J. Ralph, J. Ross, K. Baker, *et al.*, "Design of inertial fusion implosions reaching the burning plasma regime," Nature Physics **18**, 251–258 (2022).
[16] J. Lindl, S. Haan, O. Landen, A. Christopherson, and R. Betti, "Progress toward a self-consistent set of 1d ignition capsule metrics in icf," Physics of Plasmas **25** (2018).
[17] A. J. Creely, M. J. Greenwald, S. B. Ballinger, D. Brunner, J. Canik, J. Doody, T. Fülöp, D. T. Garnier, R. Granetz, T. K. Gray, and et al., "Overview of the sparc tokamak," Journal of Plasma Physics **86**, 865860502 (2020).